Journal of Trace Elements in Medicine and Biology 52 (2019) 12–17

Contents lists available at ScienceDirect

Journal of Trace Elements in Medicine and Biology

journal homepage: www.elsevier.com/locate/jtemb

# Preparation, characterizations and *in vitro* cytotoxic activity of nickel oxide nanoparticles on HT-29 and SW620 colon cancer cell lines

Shahanavaj Khan[a,b,*], Anees A. Ansari[c], Abdul Malik[d], Anis Ahmad Chaudhary[e], Jakeera Begum Syed[f], Azmat Ali Khan[g]

[a] Department of Bioscience, Shri Ram Group of College (SRGC), Muzaffarnagar 251001, India
[b] Nanomedicine & Biotechnology Research Unit, Department of Pharmaceutics, College of Pharmacy, King Saud University, Riyadh, Saudi Arabia
[c] King Abdullah Institute for Nanotechnology, King Saud University, PO Box 2455, Riyadh 11451, Saudi Arabia
[d] Department of Clinical Laboratory Science, College of Applied Medical Sciences, King Saud University, Riyadh, Saudi Arabia
[e] Department of Pharmacology, College of Medicine, Al-Imam Mohammad Ibn Saud Islamic University, Riyadh, Saudi Arabia
[f] College of Medicine and Dentistry, Dar Al Uloom University, Al Mizan St, Al Falah, Riyadh 13314, Saudi Arabia
[g] Pharmaceutical Biotechnology Laboratory, Department of Pharmaceutical Chemistry, College of Pharmacy, King Saud University, Riyadh 11451, Saudi Arabia

ARTICLE INFO

*Keywords:*
Nickel oxide nanoparticles
Cancer cell lines
MTT assay
Inverted microscopy
Cytotoxicity
Western blot assay

ABSTRACT

Despite the extensive implication of nickel oxide nanoparticles (NiO-NPs) in different fields such as biomedical science and industrial manufacturing, their effect on human cancer cells has not been elucidated. In this study, we report a simple process for the preparation of NiO-NPs. X-ray diffraction and transmission electron microscopy were used to characterize the surface architecture and dimension of the synthesized NiO-NPs. The average diameter of the NiO-NPs was approximately 20–25 nm. We used two human colon cancer cell lines, HT-29 and SW620, to assess the nanoparticles' cytotoxicity. The MTT assay showed that the NiO-NPs reduced cell viability of HT-29 and SW620 cell lines. The results of inverted microscopy showed the highest cytotoxic activity with 600 μg/ml concentration of NiO-NPs on HT-29 cells. Western blot assay showed the downregulation of anti-apoptotic Bcl2 and Bcl-xL proteins in HT-29 cells treated with NiO-NPs. Moreover the results demonstrated the induction of PARP (Cleaved) in NiO-NPs treated HT-29 cells which are considered the marker of apoptosis. The NiO-NPs were not demonstrated bactericidal effect on six different bacterial strains tested, implying that the NiO-NPs may not perturb the human normal gut microbiome. The results have showed the promising application of the NiO-NPs in management of cancer in near future.

## 1. Introduction

Nanomaterials have garnered much attention for their versatile applications [1–3]. The interdisciplinary study of nanoscience and biology provides a gateway for development and synthesis of novel nanomaterials in different fields of science [4–7]. The field of nanobiotechnology connects the chemical sciences with biological disciplines through different chemical techniques in designing new platforms for understanding biological systems and disease diagnosis and treatment [6,8]. In general, nanoparticles (NPs) are smaller than large biological molecules such as enzymes, proteins, and receptors. Our previous research demonstrated that different metal oxide NPs can exert effects on different cancer cell lines *in vitro* [9]. Metal oxide NPs, including cobalt oxide ($Co_3O_4$), manganese oxide ($Mn_3O_4$), titanium dioxide (TiO2), silver oxide ($Ag_2O$), and zinc oxide (ZnO), have been investigated for their anticancer and antibacterial activities [10–14]. The microbiome of human intestine restrains about 100 trillion bacterial strains. Different bacterial species and their metabolites play critical roles in the development of colorectal cancer (CRC). Latest reports illustrate that distress in the gut microbial population may affect the normal physiology and connect with the growth and development of numerous diseases such as cancer. The enigmatic impacts of bacterial disbiosis and cancer progression have been documented [15–17].

Several studies have shown that NPs can be cytotoxic because of their small size and high reactivity [7,18,19]. NPs can be target-specific, a characteristic that can be leveraged in developing nanodrugs for the treatment and management of different cancers [20,21]. Because of their size, NPs can be retained in various cells, tissues, and organs longer than larger-size particles [22]. Multiple studies have shown that NPs may be easily transported in the body, penetrate cell membranes,

* Corresponding author at: Department of Bioscience, Shri Ram Group of College (SRGC), Muzaffarnagar 251001, India.
*E-mail address:* khan.shahanavaj@gmail.com (S. Khan).

https://doi.org/10.1016/j.jtemb.2018.11.003
Received 21 May 2018; Received in revised form 18 October 2018; Accepted 6 November 2018
0946-672X/ 

accumulate in target sites, be retained in mitochondria, and may induce cytotoxic effects [3,23]. Using NPs to treat and manage diseases, such as cancer, offers options to potentially destroy cancer cells with minimum damage to healthy cells and tissues [24].

Studies evaluating the cytoxicity of nickel oxide NPs (NiO-NPs) in human cancer cell lines are limited. Ahamed et al. [25] reported that NiO-NP cytoxicity in HepG2 cells was mediated by reactive oxygen species (ROS). Similarly, Ada et al. [26] observed the cytotoxicity of NiO-NPs to cervix epithelioid carcinoma (HeLa) cells. However, the principal molecular mechanism of apoptosis in HT-29 and SW620 human colon cancer cells following exposure to NiO-NPs is unclear. Therefore, we focused on developing smaller (> 100 nm) NiO-NPs and investigated their effects on colon cancer cells. We analyzed alterations in proteins regulating apoptosis. In addition, we evaluated the antibacterial activity of NiO-NPs against different strains of gram-positive and gram-negative bacteria.

## 2. Materials and methods

### 2.1. Consumables and reagents

Nickel nitrate ammonia hydroxide, ethylene glycol, 3-(4,5- dimethylthiazol-2-yl)-2, 5-diphenyltetrazolium bromide (MTT reagent), and anti-β-actin antibody were purchased from Sigma-Aldrich (St. Louis, MO, USA). Dulbecco's modified Eagle's medium (DMEM), fetal bovine serum (FBS), trypsin, and penicillin-streptomycin were obtained from Invitrogen (Carlsbad, CA, USA). Human colon cancer cell lines HT-29 and SW620 were purchased from the American Type Culture Collection (ATCC; Manassas, VA, USA). Antibodies for Bcl2 and Bcl-xL and secondary antibodies labeled with horseradish peroxidase, RIPA buffer, and sodium dodecyl sulfate (SDS) were procured from Santa Cruz Biotechnology (Dallas, TX, USA). All other chemicals and reagents used in the experiments were of the highest quality and obtained from commercial sources.

### 2.2. Synthesis of NiO-NPs

Nickel nitrate and ethylene glycol were used as starting precursors without any further purification. Aqueous dissolved nickel nitrate was mixed in ethylene glycol, and the solution was maintained on a hot plate with constant stirring at 100 °C for 2 h [27]. A minimum amount of ammonium hydroxide was added to the reaction for precipitation. The gray precipitate was centrifuged and rinsed several times with distilled water to remove excess amounts of ammonium and nitrate ions and then dried at 100 °C.

### 2.3. Characterizations of NiO-NPs

#### 2.3.1. X-ray powder diffraction (XRD) for particle size measurement

The crystallinity of the powder samples was examined by XRD at room temperature using a PANalytical X'Pert X-ray diffractometer equipped with a nickel filter using Cu-K alpha (λ = 1.54056 Å) radiation as the X-ray source.

#### 2.3.2. Transmission electron microscopy (TEM) for NiO-NPs

The test samples were formulated by dropping the suspension of NiO-NPs onto a TEM copper grid and dehydrating at room temperature. Three TEM samples were formulated, and five micrographs of each sample were studied to analyze the collective mean of the particle size. Sample size and morphology were inspected using a field emission transmission electron microscope (FETEM, JEM-2100 F, JEOL, Japan) operating at an accelerating voltage of 200 kV.

Evaluation of cytotoxicity of NiO-NPs.

### 2.4. Cell culture

HT-29 and SW620 cells were obtained from the American Type Culture Collection (ATCC, Manassas, VA, USA). SW620 human colon cancer cells were cultured in DMEM supplemented with 5% glutamine, 100 U/mL penicillin-streptomycin, and 10% FBS at 37 °C in an incubator with 5% $CO_2$. The cells were harvested with 0.25% trypsin when confluence reached 85%, and were used to sub-culture into large-volume 25 $cm^2$ flasks or 96-well plates as required for the experiments.

#### 2.4.1. Treatment of cells with NiO-NPs

The NiO-NP dry powder was suspended in DMEM and serially diluted to 2.5, 5, 10, 20, 40, 80, 160, 320 and 640 μg/mL. These concentrations were then sonicated at room temperature at 40 W for 15 min to avoid NP agglomeration prior to treatment. Untreated cells served as controls.

#### 2.4.2. Evaluation of cytotoxicity of NiO-NPs

The MTT-based cell viability assay was performed to determine the cytotoxicity of NiO-NPs as outlined by Mosmann [28]. HT-29 and SW620 cells were incubated at 37 °C for 24 h to attach to the surface of 96-well plates prior to NiO-NP exposure. This assay analyzes the function of mitochondria by determining the potential of viable cells to reduce MTT to formazan. HT-29 and SW620 cells ($1 \times 10^4$) were seeded in each well of 96-well plates and treated with different concentrations of NiO-NPs (2.5, 5, 10, 20, 40, 80, 160, 320 and 640 μg/mL), then incubated at 37 °C for 24 h.

HT-29 cells were also treated with serial concentrations of the anticancer drug doxorubicin for 24 h at 37 °C and 5% $CO_2$. Untreated cells (control group) were exposed to 200 μL of culture medium without NiO-NPs or doxorubicin in each experiment. At the end of the treatment period, the culture medium was replaced with fresh medium containing MTT solution and incubated at 37 °C for 3 h until the development of purple formazan. The formazan product was solubilized in isopropanol. Next, the plates were centrifuged for 5 min at 2300 × g to allow the cell debris and the remaining NiO-NPs to settle. Finally, 100 μL of the supernatant were pipetted to a new 96-well plate, and the absorbance was measured at 570 nm with a microplate reader (ELx800, BioTek, USA). All tests were performed in triplicate. The replicates were averaged to calculate the $IC_{50}$ value and cell survival percentages.

### 2.5. Inverted microscopy for the analysis of any morphological change in HT-29 cells

Crystal violet staining was performed for the estimation of anti-carcinomas activities in NiO-NPs through observation of change in morphology of treated HT-29 cells as published protocol in our recent study [26]. HT-29 cells were cultured in DMEM as demonstrated in method section. Various concentrations of NiO-NPs and HT-29 cell suspensions were mixed, plated in 6-well culture plate (Becton, Dickinson and Co., Franklin Lakes, NJ, USA) and incubated at 37 °C for 24 h. The extra stain of dye was rinsed properly using distilled water until no superfluous dye leached from the wells of culture plate. The morphology of cells was analyzed under an inverted microscope using Microvisiable software on Micros at 20 × . Moreover, expression profile of anti-apoptotic Bcl-2, Bcl-xL and β-actin (control) were estimated by western blot assay.

### 2.6. Estimation of effect of NiO-NPs on anti-apoptotic proteins

We used western blotting to determine changes in the expression of genes encoding Bcl2 and Bcl-xL, along with the positive control β-actin. HT-29 cells were grown in DMEM containing 5% glutamine, 100 U/mL penicillin-streptomycin, and 10% FBS at 37 °C in an incubator with 5% $CO_2$. Approximately 60–70% confluent HT-29 human colon cancer cells were exposed to 10 μg/mL NiO-NP suspension for 24 h. Following

treatment, whole-cell lysates were produced with freshly prepared lysis buffer as previously described [11,29]. Alterations in expression were determined using anti-BclxL, anti-Bcl2 (Santa Cruz Biotechnology), and anti-β-actin (Sigma-Aldrich) antibodies and the development of immune blots. Reactivity was analyzed using horseradish peroxidase-conjugated secondary antibodies and chemiluminescence reagents (GE Healthcare, Little Chalfont, UK). A molecular imager was used to capture and quantify the immunoreactive bands.

### 2.7. Estimation of apoptosis by the analysis of poly (ADP-ribose) polymerase (PARP) (cleaved)

HT-29 cells were grown as illustrated in our published study [10]. The cultured HT-29 cells were treated with 5 µg/mL and 10 µg/mL NiO-NPs concentrations of NiO-NPs for 24 h. Untreated cells were used as control. The soluble proteins were observed using anti-PARP antibody with a dilution of 1:500 (BioVision), and anti-β-actin (internal control) with a dilution of 1:10,000 (Sigma) through immuno-blot technique. The reactivity of PARP (Cleaved) and anti-β-actin was determined by secondary antibody conjugated with horseradish peroxidase and clarity ECL substrate for chemiluminescence using C-Digit Blot Scanner.

### 2.8. Estimation of NiO-NP antibacterial activity

The antibacterial activity of NiO-NPs was measured using a disk diffusion method with three gram-positive and three gram-negative bacterial strains [29].

#### 2.8.1. Selection of bacterial strains

We selected *Bacillus subtilis*, *Staphylococcus aureus*, and *Enterococcus faecalis* (gram-positive) and *Proteus vulgaris*, *Salmonella typhimurium*, and *Shigella sonnei* (gram-negative) to test the antibacterial properties of NiO-NPs. Mueller-Hinton broth was used for sub-culturing bacteria from pure cultures at 37 °C for 18 h. The turbidity was adjusted to approximately 0.5 McFarland standard in each culture. The bacterial strains were grown on separate agar plates. Sterile paper disks were placed on the surface of the agar in all experimental plates. A 10-µL suspension of NiO-NPs with a concentration of 250 µg/mL was used in the experiments.

#### 2.8.2. Evaluation of minimal inhibitory concentration (MIC)

The MIC of the NiO-NPs was evaluated along with positive-control drugs cefotaxime MIC test strips [Liofilchem, Roseto Degli Abruzzi, Italy] and ampicillin [BioMérieux, Marcy-l'Étoile, France] using a standard CLSI protocol [29]. All culture plates were incubated at 37 °C for 18 h. The experiments to quantify MIC values were performed in triplicate. The transparent area was measured as the zone of inhibition around the disks and used for comparison with standards.

### 2.9. Statistical analysis

All experiments of MTT assay were performed in triplicate for statistical analysis. Data are presented as mean ± the standard deviation. Differences between groups were estimated using one-way analysis of variance followed by Dunnett's post hoc test. $p < 0.05$ was considered statistically significant.

## 3. Results and discussion

### 3.1. Synthesis of NiO-NPs

NiO-NPs were synthesized successfully using nickel nitrate and ethylene glycol.

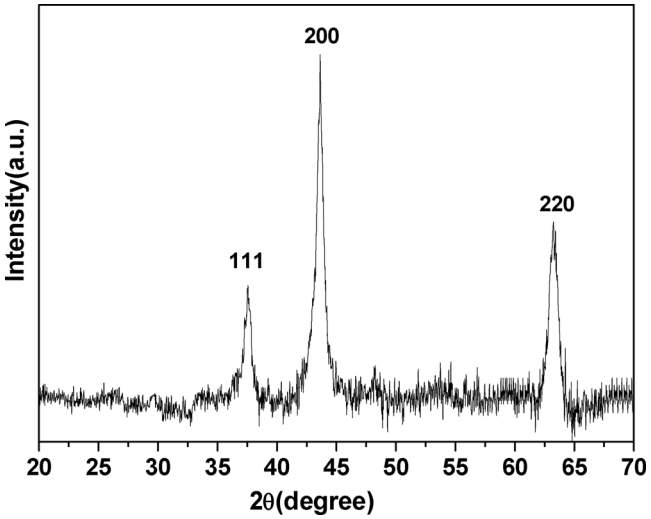


**Fig. 1.** X-ray diffraction pattern of nickel oxide nanoparticles. X-ray diffraction pattern of Nickel oxide nanoparticles.

### 3.2. Characterization of NiO-NPs

The crystallographic and morphological structure of synthesized NiO-NPs was characterized using XRD and TEM.

#### 3.2.1. X-ray powder diffraction (XRD) for particle size measurement

Phase purity, crystallinity, and crystal structure of the products were determined from XRD patterns. As shown in Fig. 1, all principle reflection peaks correspond to the specific (111), (200), and (220) planes, which are consistent with the cubic structure of NiO in the standard data (JCPDS card no. 47-1049) [30,31]. The peak position and intensity of the diffraction planes matched the data in published reports. None of the peaks corresponded to any impurity phase of nickel hydroxide or salt, and thus we ruled out the formation of a secondary phase. All diffraction peaks were broad, clearly indicating the nanocrystalline behavior of the NiO-NPs. The average crystallite size of the sample was calculated from X-ray line broadening of the peaks at the (200) and (220) planes using the Debye-Scherrer equation.

#### 3.2.2. Transmission electron microscopy (TEM) for NiO-NPs

Fig. 2 shows the FETEM image of NiO-NPs. The NPs are irregular in shape and size, with a narrow size distribution (average particle size 20–25 nm), and slightly aggregated. The average crystalline size of the NiO-NPs closely matches the average particle size calculated by the

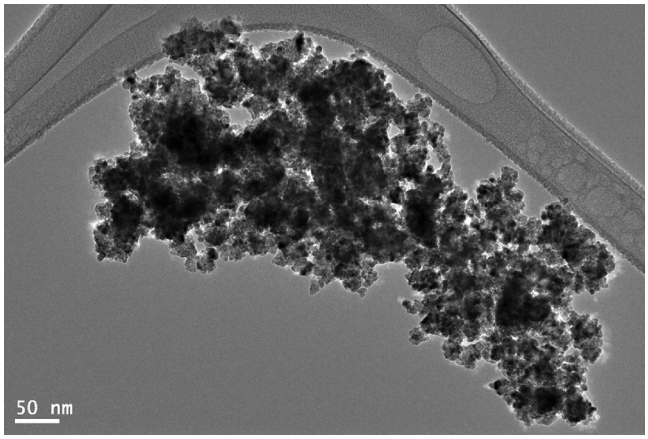


**Fig. 2.** Micrograph of Nickel oxide nanoparticles (field emission transmission electron microscopy).

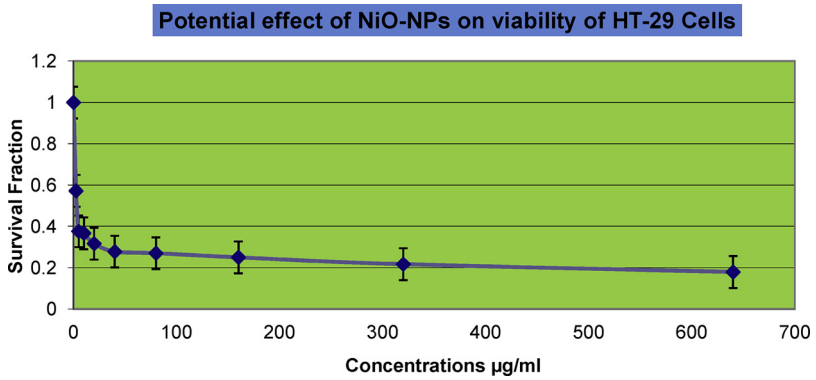


**Fig. 3.** Effect of nickel oxide nanoparticles (2.5–640 µg/mL) on viability of HT-29 cells following a 24-h treatment. Error bars denote standard deviation (n = 3).

Debye-Scherrer equation from the XRD pattern.

### 3.3. Evaluation of cytotoxicity of NiO-NPs

The MTT assay was performed following a 24-h exposure of NiO-NPs on HT-29 and SW620 cells. Different concentrations of NiO-NPs induced cytotoxicity in HT-29 and SW620 cells (Figs. 3 and 4, respectively). More significant cytotoxic response was observed in HT-29 cells following exposure to NiO-NPs with dose depend manner (Fig. 3). The highly resistant SW620 cells exhibited a much higher survival fraction (Fig. 4). The untreated HT-29, SW620 (negative control) cells exposed with various concentrations (0, 2.5, 5, 10, 20, 40, 80, 160, 320 and 640 µg/mL) of NiO-NPs were not demonstrated considerable cytotoxic activity after an incubation of 24 h. The synthesized NiO-NPs yielded $IC_{50}$ values of 13.72 and 394.41 µg/mL for HT-29 and SW620 cells, respectively. These outcomes clearly illustrate that NiO-NPs are more cytotoxic to HT-29 cells at lower doses, indicating therapeutic potential. A significant cytotoxicity was shown by the control drug doxorubicin, as in our previous report (data not shown) [29].

### 3.4. Inverted microscopy for the analysis of any morphological change in HT-29 cells

The possible alterations in morphology of HT-29 cells were observed by inverted microscopy using crystal violet staining assay against various concentrations of NiO-NPs. The inverted microscopy results were evidently illustrated decline in numbers of cells of HT-29 with various concentration of NiO-NPs with respect to control (untreated) cells (Fig. 5A–D). The images of inverted microscopy showed shrinkage, cytoplasmic condensation and loss of membrane integrity in treated HT-29 cells with respect to untreated cells. The results of inverted microscopy demonstrate that NiO-NPs inhibit cellular proliferation of HT-29 cells by stimulating the process of cell death.

### 3.5. Estimation of effect of NiO-NPs on anti-apoptotic proteins

Western blot analysis showed a downregulation in Bcl-2 and Bcl-xL (Fig. 6A and 6B), whereas the expression of the internal control β-actin did not change significantly in the HT-29 cells treated with NiO-NPs (Fig. 6C). The findings indicate that the downregulation of the anti-apoptotic Bcl-2 and Bcl-xL may have induced apoptosis in the HT-29 cells by interacting with key proteins of the programmed cell death pathway, such as Bax, Mcl-1, and p53 [32,33]. Therefore, the NiO-NPs under study have the potential to promote the apoptosis.

### 3.6. Estimation of apoptosis by the analysis of poly (ADP-ribose) polymerase (PARP) (cleaved)

Poly (ADP-ribose) polymerase-1 (PARP-1; 116 kDa) cleavage into PARP (89 kDa molecular weight) through caspases allowing DNA damage is supposed as a potential distinctive marker of apoptosis [34]. The results of our current study demonstrated the induction of PARP (Cleaved) in HT-29 cells treated with different concentration of NiO-NPs in comparison to control cells (7 A). β-actin was as a internal control in the experiment (Fig. 7B). PARP is an important protein of apoptosis which helps in regulation of different cellular processes including programmed cell death and DNA repair. PARP can be stimulated during cellular stress and DNA damage responses.

### 3.7. Estimation of NiO-NP antibacterial activity

The antibacterial activity of NiO-NPs was assessed against six bacterial strains, along with that of drugs used as controls. The NiO-NPs did not exhibit significant antibacterial activity against any bacterial strain tested at a concentration of 250 µg/mL, unlike the cefotaxime and ampicillin used as positive controls.

Ampicillin exhibited lower antibacterial activity than cefotaxime towards all bacterial strains tested. The minimal inhibitory concentration (MIC) value of NiO-NPs was > 10 mg/mL (Supplementary Table

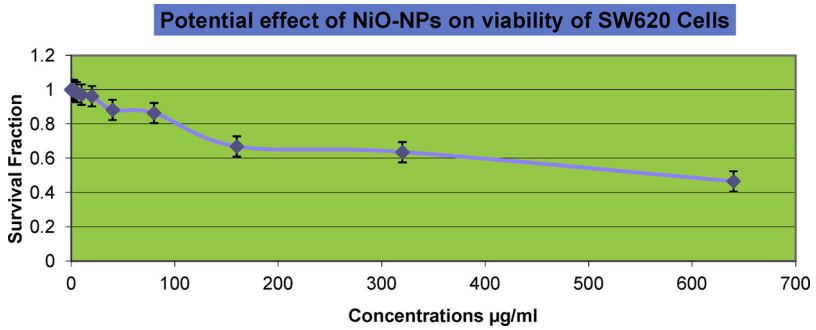


**Fig. 4.** Effect of nickel oxide nanoparticles (2.5–640 µg/mL) on viability of SW620 cells following a 24-h treatment. Error bars denote standard deviation (n = 3).

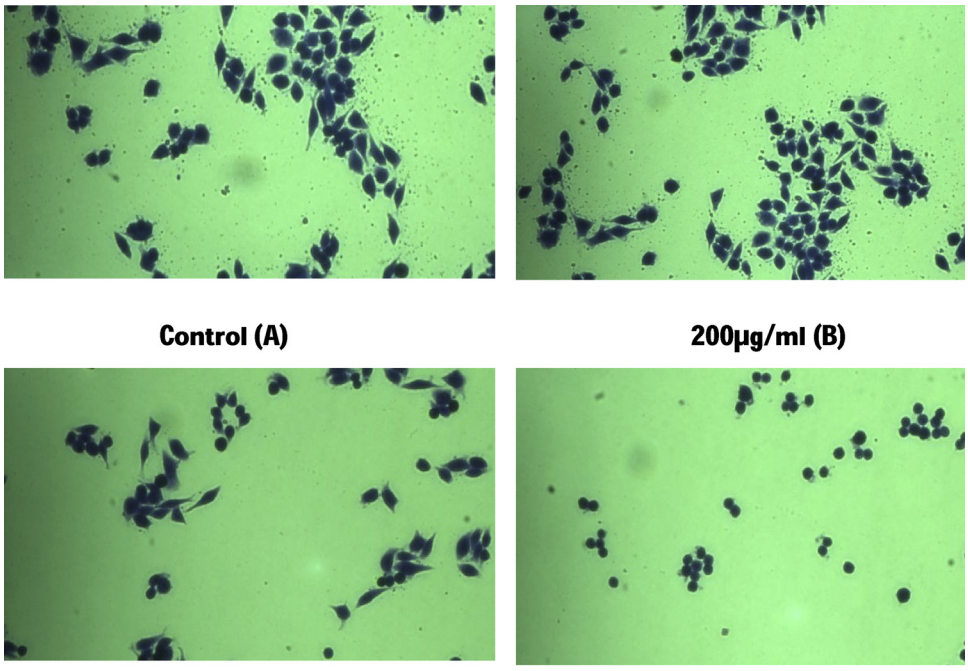


**Fig. 5.** Morphological alterations and decline in number of the HT-29 cell demonstrates the cytotoxic activity of nickel oxide nanoparticles with respect to control (untreated) cells. Images 5A-5D showed HT-29 cells exposed with different concentrations of nickel oxide nanoparticles. The photographs were taken using Microvisible software after crystal violet staining.

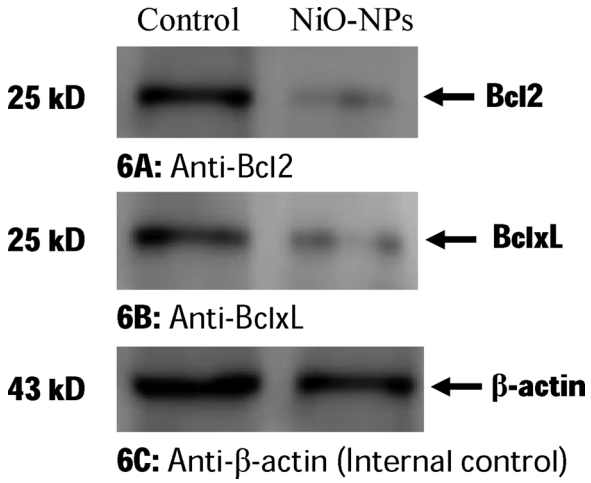


**Fig. 6.** Western blot assay showed NiO-NPs mediated apoptosis in HT-29 cell line. (A) Inhibition of expression of Bcl-2 indicated on the immuno-blot with compression to positive control. (B) Inhibition of expression of Bcl-xL indicated on the immuno-blot with compression to positive control. (C) β-actin (Internal control) illustrated no any effect on the immuno-blot in compression to untreated control.

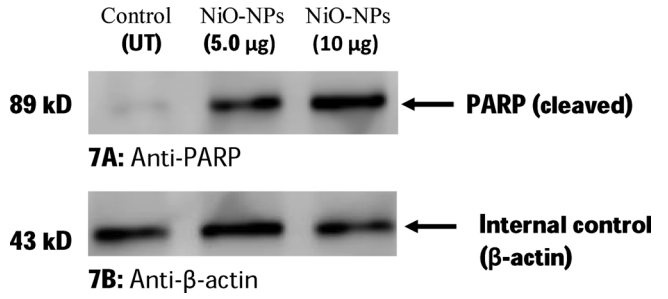


**Fig. 7.** Images illustrated the induction of PARP (Cleaved) in HT-29 cells treated with 5.0 µg and 10 µg concentrations of NiO-NPs with compression to untreated control (7 A). β-actin was used as internal control in the current study (7B).

S1). The role of microbiota in health and disease has become a topic of investigation over the past decade. Alterations in the quantities and species of microbiota present in the human body may contribute to the risk of infection, leading to various diseases, including cancer [16,17]. An ideal anticancer drug or nanoparticle should not disrupt the normal human microbiome. We found non-significant bactericidal effects of NiO-NPs in terms of the MIC values. Therefore, NiO-NPs could be used in biomedical applications, including treatment of cancer, conceivably without disturbing the balance of the gut microbiome.

## 4. Conclusion

In the present study, we synthesized and characterized NiO-NPs with an irregular spherical shape and diameter of approximately 20–25 nm. The NiO-NPs significantly reduced the viability of HT-29 and SW620 human colon cancer cells. The results of inverted microscopy were clearly demonstrated the cytotoxic activity of NiO-NPs with comparison to untreated control cells through decline in numbers and alteration in morphology of treated HT-29 cells. Moreover, Bcl-2 and Bcl-xL protein levels were downregulated, suggesting that NiO-NPs can induce cell death through alterations of the mitochondrial pathway of apoptosis. The outcome of our current study showed the induction of PARP (Cleaved) in HT-29 cells. PARP is a very crucial protein of apoptosis that may involved to control various cellular processes such as programmed cell death and DNA repair. Our data collectively suggest that NiO-NPs maybe involved as a treatment option in colorectal cancer patients. The NiO-NPs did not exert significant bactericidal effects on six bacterial strains. Further research is required to determine whether NiO-NPs would be suitable as agents for the management and treatment of different types of cancer. To our knowledge, this is the first report showing that NiO-NPs can induce cytotoxicity in HT-29 and SW620 cells by altering the level of apoptotic regulatory proteins.

## Conflict of interest

The authors declare that they do not have any potential conflict of interest related to the present study.

## Acknowledgements

The authors are thankful to the Research Center at the College of Applied Medical Sciences, and Deanship of Scientific Research, King Saud University for funding this work.

## Appendix A. Supplementary data

Supplementary material related to this article can be found, in the online version, at doi:https://doi.org/10.1016/j.jtemb.2018.11.003.

## References

[1] N. Nishiyama, Nanomedicine: nanocarriers shape up for long life, Nat. Nanotechnol. 2 (2007) 203–204.
[2] D. Peer, J.M. Karp, S. Hong, O.C. Farokhzad, R. Margalit, R. Langer, Nanocarriers as an emerging platform for cancer therapy, Nat. Nanotechnol. 2 (2007) 751–760.
[3] A. Nel, T. Xia, L. Madler, N. Li, Toxic potential of materials at the nanolevel, Science 311 (2006) 622–627.
[4] N. Golbamaki, B. Rasulev, A. Cassano, R.L. Marchese Robinson, E. Benfenati, J. Leszczynski, et al., Genotoxicity of metal oxide nanomaterials: review of recent data and discussion of possible mechanisms, Nanoscale 7 (2015) 2154–2198.
[5] H.L. Karlsson, A.R. Gliga, F.M. Calleja, C.S. Goncalves, I.O. Wallinder, H. Vrieling, et al., Mechanism-based genotoxicity screening of metal oxide nanoparticles using the ToxTracker panel of reporter cell lines, Part Fibre Toxicol. 11 (2014) 41.
[6] C.R. Lowe, Nanobiotechnology: the fabrication and applications of chemical and biological nanostructures, Curr. Opin. Struct. Biol. 10 (2000) 428–434.
[7] W.H. De Jong, P.J. Borm, Drug delivery and nanoparticles:applications and hazards, Int. J. Nanomed. 3 (2008) 133–149.
[8] G.M. Whitesides, The' right' size in nanobiotechnology, Nat. Biotechnol. 21 (2003) 1161–1165.
[9] S. Khan, A.A. Ansari, A.A. Khan, M. Abdulla, O. Al-Obaid, R. Ahmad, In vitro evaluation of cytotoxicity, possible alteration of apoptotic regulatory proteins, and antibacterial activity of synthesized copper oxide nanoparticles, Colloids Surf. B Biointerfaces 153 (2017) 320–326.
[10] S. Khan, A.A. Ansari, A.A. Khan, R. Ahmad, O. Al-Obaid, W. Al-Kattan, In vitro evaluation of anticancer and antibacterial activities of cobalt oxide nanoparticles, J. Biol. Inorg. Chem. 20 (2015) 1319–1326.
[11] S. Khan, A.A. Ansari, A.A. Khan, M. Abdulla, O. Al-Obaid, R. Ahmad, In vitro evaluation of anticancer and biological activities of synthesized manganese oxide nanoparticles, Med. Chem. Res. 7 (2016) 1647–1653.
[12] Q. Saquib, A.A. Al-Khedhairy, M.A. Siddiqui, F.M. Abou-Tarboush, A. Azam, J. Musarrat, Titanium dioxide nanoparticles induced cytotoxicity, oxidative stress and DNA damage in human amnion epithelial (WISH) cells, Toxicol. In Vitro 26 (2012) 351–361.
[13] A.R. Gliga, S. Skoglund, I.O. Wallinder, B. Fadeel, H.L. Karlsson, Size-dependent cytotoxicity of silver nanoparticles in human lung cells: the role of cellular uptake, agglomeration and Ag release, Part. Fibre Toxicol. 11 (2014) 11.
[14] Z. Han, Q. Yan, W. Ge, Z.G. Liu, S. Gurunathan, M. De Felici, et al., Cytotoxic effects of ZnO nanoparticles on mouse testicular cells, Int. J. Nanomed. 11 (2016) 5187–5203.
[15] K. Shahanavaj, I. Gil-Bazo, M. Castiglia, G. Bronte, F. Passiglia, A.P. Carreca, et al., Cancer and the microbiome: potential applications as new tumor biomarker, Expert Rev. Anticancer Ther. 15 (2015) 317–330.
[16] S. Khan, Potential role of Escherichia coli DNA mismatch repair proteins in colon cancer, Crit. Rev. Oncol. Hematol. 96 (2015) 475–482.
[17] J.C. Arthur, E. Perez-Chanona, M. Muhlbauer, S. Tomkovich, J.M. Uronis, T.J. Fan, et al., Intestinal inflammation targets cancer-inducing activity of the microbiota, Science 338 (2012) 120–123.
[18] E. Perez-Herrero, A. Fernandez-Medarde, Advanced targeted therapies in cancer: Drug nanocarriers, the future of chemotherapy, Eur. J. Pharm. Biopharm. 93 (2015) 52–79.
[19] M. Estanqueiro, M.H. Amaral, J. Conceicao, J.M. Sousa Lobo, Nanotechnological carriers for cancer chemotherapy: the state of the art, Colloids Surf. B Biointerfaces 126 (2015) 631–648.
[20] C. Haglund, A. Aleskog, P. Nygren, J. Gullbo, M. Hoglund, M. Wickstrom, et al., In vitro evaluation of clinical activity and toxicity of anticancer drugs using tumor cells from patients and cells representing normal tissues, Cancer Chemother. Pharmacol. 69 (2012) 697–707.
[21] D. McShan, P.C. Ray, H. Yu, Molecular toxicity mechanism of nanosilver, J. Food Drug Anal. 22 (2014) 116–127.
[22] A.E. Porter, M. Gass, J.S. Bendall, K. Muller, A. Goode, J.N. Skepper, et al., Uptake of noncytotoxic acid-treated single-walled carbon nanotubes into the cytoplasm of human macrophage cells, ACS Nano 3 (2009) 1485–1492.
[23] A. Avalos, A.I. Haza, D. Mateo, P. Morales, Interactions of manufactured silver nanoparticles of different sizes with normal human dermal fibroblasts, Int. Wound J. 13 (2016) 101–109.
[24] Y.N. Wu, D.H. Chen, X.Y. Shi, C.C. Lian, T.Y. Wang, C.S. Yeh, et al., Cancer-cell-specific cytotoxicity of non-oxidized iron elements in iron core-gold shell NPs, Nanomedicine 7 (2011) 420–427.
[25] M. Ahamed, D. Ali, H.A. Alhadlaq, M.J. Akhtar, Nickel oxide nanoparticles exert cytotoxicity via oxidative stress and induce apoptotic response in human liver cells (HepG2), Chemosphere 93 (2013) 2514–2522.
[26] K. Ada, M. Turk, S. Oguztuzun, M. Kilic, M. Demirel, N. Tandogan, et al., Cytotoxicity and apoptotic effects of nickel oxide nanoparticles in cultured HeLa cells, Folia Histochem. Cytobiol. 48 (2010) 524–529.
[27] Q. Li, F. Wang, L. Sun, Z. Jiang, T. Ye, M. Chen, et al., Design and Synthesis of Cu@CuS Yolk–Shell Structures with Enhanced Photocatalytic Activity ncbi, Nano-Micro Lett. 9 (2017) 1–9.
[28] T. Mosmann, Rapid colorimetric assay for cellular growth and survival: application to proliferation and cytotoxicity assays, J. Immunol. Methods 65 (1983) 55–63.
[29] S. Khan, A.A. Ansari, A.A. Khan, W. Al-Kattan, O. Al-Obeedd, A. Rehan, Design, synthesis and in vitro evaluation of anticancer and antibacterial potential of surface modified Tb(OH)3@SiO2 core–shell nanoparticles, RSC Adv. 6 (2016) 18667–18677.
[30] S. Xiong, C. Yuan, B. Zhang, Q. Y, Mesoporous NiO with various hierarchical nanostructures by quasi-nanotubes/nanowires/nanorods self-assembly: controllable preparation and application in supercapacitors, CrystEngComm 13 (2011) 626–632.
[31] J. Park, E. Kang, S.U. Son, H.M. Park, M.K. Lee, J. Kim, et al., Monodisperse nanoparticles of Ni and NiO: synthesis, characterization, self-assembled superlattices, and catalytic applications in the suzuki coupling reaction, Adv. Mater. 17 (2005) 429–434.
[32] M.T. Hemann, S.W. Lowe, The p53-Bcl-2 connection, Cell Death Differ. 13 (2006) 1256–1259.
[33] S. Khan, A.A. Ansari, C. Rolfo, A. Coelho, M. Abdulla, K. Al-Khayal, et al., Evaluation of in vitro cytotoxicity, biocompatibility, and changes in the expression of apoptosis regulatory proteins induced by cerium oxide nanocrystals, Sci. Technol. Adv. Mater. 18 (2017) 364–373.
[34] L. Ge, Q. Li, M. Wang, J. Ouyang, X. Li, M.M. Xing, Nanosilver particles in medical applications: synthesis, performance, and toxicity, Int. J. Nanomed. 9 (2014) 2399–2407.